PHILOSOPHICAL TRANSACTIONS OF THE ROYAL SOCIETY A MATHEMATICAL, PHYSICAL & ENGINEERING SCIENCES

The Ophiolites of the Tibetan Geotraverses, Lhasa to Golmud (1985) and Lhasa to Kathmandu (1986)

Julian A. Pearce and Deng Wanming

Phil. Trans. R. Soc. Lond. A 1988 **327**, 215-238
doi: 10.1098/rsta.1988.0127

Phil. Trans. R. Soc. Lond. A **327**, 215–238 (1988) [215]
Printed in Great Britain

The ophiolites of the Tibetan Geotraverses, Lhasa to Golmud (1985) and Lhasa to Kathmandu (1986)

By Julian A. Pearce[1] and Deng Wanming[2]

[1] *Department of Geology, University of Newcastle-upon-Tyne, Newcastle-upon-Tyne, U.K.*
[2] *Institute of Geology, Academia Sinica, Beijing, People's Republic of China*

Ophiolite belts are found in Tibet along the Zangbo, Banggong and Jinsha River Sutures and in the Anyemaqen mountains, the eastern extension of the Kunlun mountains. Where studied, the Zangbo Suture ophiolites are characterized by: apparently thin crustal sequences (3–3.5 km); an abundance of sills and dykes throughout the crustal and uppermost mantle sequences; common intraoceanic melanges and unconformities; and an N-MORB petrological and geochemical composition. The ophiolites probably formed within the main neo-Tethyan ocean and the unusual features may be due to proximity to ridge-transform intersections, rather than to genesis at very slow-spreading ridges as the current consensus suggests. The Banggong Suture ophiolites have a supra-subduction zone petrological and geochemical composition – although at least one locality in the Ado Massif shows MORB characteristics. However, it is also apparent that the dykes and lavas show a regional chemical zonation, from boninites and primitive island arc tholeiites in the south of the ophiolite belt, through normal island arc tholeiites in the central belt to island arc tholeiites transitional to N-MORB in the north. The ophiolites could represent fragments of a fore-arc, island arc, back-arc complex developed above a Jurassic, northward-dipping subduction zone and emplaced in several stages during convergence of the Lhasa and Qiangtang terranes. The ophiolites of the Jinsha River Suture have a N-MORB composition where analysed, but more information is needed for a proper characterization. The Anyemaqen ophiolites, where studied, have a within-plate tholeiite composition and may have originated at a passive margin: it is not, however, certain whether true oceanic lithosphere, as opposed to strongly attenuated continental lithosphere, existed in this region.

1. Introduction

Ophiolites in Tibet are found in association with each of the three sutures: the Palaeogene Zangbo Suture between the Himalayan and Lhasa Terranes; the Cretaceous Banggong Suture between the Lhasa and Qiangtang Terranes; and the Triassic Jinsha River Suture between the Qiangtang and Kunlun terranes (figure 1). A fourth ophiolite belt, in the Anyemaqen mountains of northeast Tibet, has been used to invoke a possible Triassic Suture within the Kunlun Terrane, a hypothesis rejected by the Geotraverse team (Chang *et al.* 1986) owing to the absence of ophiolites within the Kunlun mountains themselves. The ophiolites of the Banggong Suture were studied and sampled at a reconnaissance level during the 1985 Geotraverse from Lhasa to Golmud; during the same Geotraverse we attempted, but failed, to reach on horseback the nearest ophiolite exposure on the Jinsha River Suture (about 100 km from the Lhasa–Golmud highway); geological observations and sample collection were subsequently carried out for us by the Geological Team of Qinghai Province. The ophiolites of the Zangbo Suture were briefly

examined during the short 1986 Geotraverse, from Lhasa to Kathmandu, although one of us (Deng) had previously worked in the area as part of a Chinese Academy of Sciences research team and provided additional material for this study. To complete the study we examined geological maps and analysed samples collected by the Chinese Academy of Sciences from the Anyemaqen ophiolite belt.

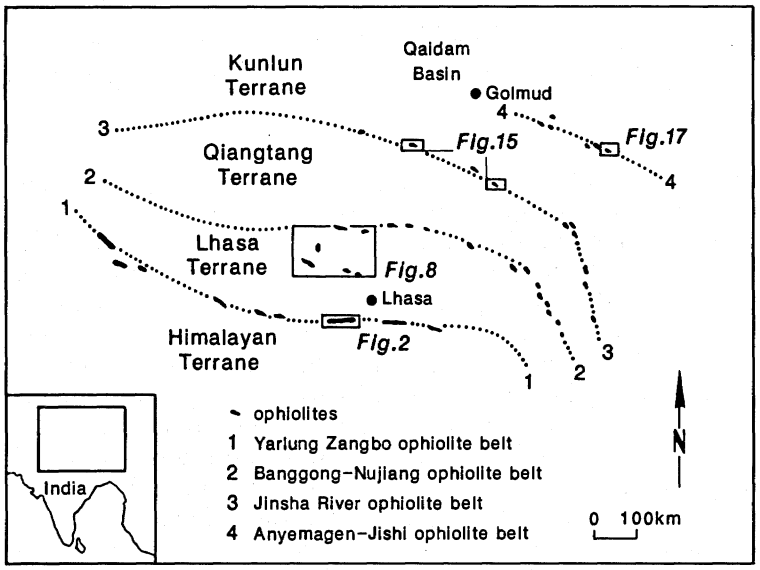

FIGURE 1. Map of Tibet showing the Geotraverse route, the main Suture zones and ophiolite belts and the location of figures 2, 8, 15 and 17.

A considerable quantity of information on the ophiolites of the Zangbo and Banggong sutures has already been published by the Chinese Academy of Sciences (e.g. Wu & Deng 1980; Deng & Zhou 1982; Deng *et al.* 1984, 1985) and the Chinese–French collaborative project (e.g. Girardeau *et al.* 1984, 1985*a*, *b*, *c*; Göpel *et al.* 1984). The aim of this chapter is briefly to summarize existing work on the ophiolite belts and to present new observations and data on this geology and geochemistry. The results will then be used to evaluate the nature of the oceanic lithosphere that separated Tibetan continental terranes prior to the Triassic, Cretaceous and Tertiary continent collision events. Emplacement mechanisms are discussed separately by Coward *et al.*, Kidd *et al.* and Dewey *et al.* (this volume).

2. METHODOLOGY

In order fully to interpret the fragments of oceanic lithosphere found within ophiolite terranes, it is necessary to determine whether that lithosphere formed at a major ridge, at a plume-related ridge, in an incipient ocean or in one of the various types of marginal basin; it is also important to recognize lithosphere that formed at or near ridge-transform intersections and whether off-axis, as well as on-axis, magmatic products are present. To carry out such an interpretation, it is necessary to combine geological, petrological and geochemical evidence to distinguish the various alternative hypotheses. The petrological and geochemical approaches used in this paper are as follows.

(1) The data on lavas, dykes and sills have been plotted on two types of diagram. The first includes MORB-normalized trace element diagrams, chondrite-normalized rare-earth patterns and Th–Ta–Hf (Wood *et al.* 1979) and Ti–Zr–Y (Pearce & Cann 1973) discrimination diagrams. These diagrams have been used to identify the nature of the magma source region and thus to distinguish between a supra-subduction zone (ssz) origin, in which Th has been selectively enriched with respect to Ta, a plume-related mid-ocean ridge basalt (P-MORB) origin, in which all incompatible elements have been enriched, and a normal mid-ocean ridge basalt (N-MORB) origin, which shows no trace element enrichment; the same diagrams can also be used to identify island arc and within-plate seamounts and aseismic ridges which may also be present in ophiolite terranes (cf. Pearce & Mei, this volume). The second type of diagram is based on plots of compatible versus incompatible elements and includes Y–Cr (Pearce 1982), Ti–Cr (Pearce 1975) and FeO/MgO–TiO_2 (Glassley 1974). These diagrams can be interpreted in terms of partial melting and crystallization histories, and thus also to distinguish MORB from ssz compositions, the former having higher concentrations of the incompatible element for a given compatible element concentration (Pearce *et al.* 1984).

(2) Of all the plutonic rocks, plagiogranites and any isotropic gabbros were analysed and interpreted as indicated above to determine intrusive setting. Cumulate rocks cannot be treated in this way because crystal cumulation distorts trace element ratios. However, order of crystallization gives some indication of tectonic setting: MORB compositions typically give an order of crystallization olivine, plagioclase, clinopyroxene, whereas ssz compositons give olivine, clinopyroxene, plagioclase (if tholeiitic) and olivine, orthopyroxene, clinopyroxene or olivine, clinopyroxene, orthopyroxene if boninitic (Pearce *et al.* 1984). In addition, microprobe analyses of clinopyroxenes can be used to identify the tectonic setting of cumulate rocks as well as clinopyroxene–phyric dykes and lavas (e.g. Nisbet & Pearce 1977; Leterrier *et al.* 1982).

(3) For the tectonized ultramafic rocks, chrome spinels are the best indicators of tectonic environment, ssz compositions showing higher Cr#(100 . Cr/(Cr+Al) ratios) than MORB compositions due to their higher degree of melting or melting of a more depleted mantle source (Dick & Bullen 1984).

Of the samples chosen for whole rock analysis some (the 'G' numbers in tables 1 and 2) have been analysed in Newcastle for major elements by atomic absorption, for the trace elements, Cr, V, Ni, Cu and Zn also by atomic absorption and for the trace elements Zr, Y, Nb, Rb and Sr by X-ray fluorescence; a subset of these samples has also been analysed for rare-earth elements (REE), Th, Ta, Hf, Sc and Co by instrumental neutron activation analysis (INAA) at the Open University. The precise location of these samples is given in Kidd *et al.*, this volume (field maps, Microfiche 2, in pocket). A second set of samples ('NI' numbers) was provided by Cao Ronglong (Guiyang) and has been analysed by the same procedures. The remaining samples have been analysed at the Institute of Geology in Beijing for the major elements and for the trace elements Zr, Y, Sr, Ba, Cr, V, Ni, Co, Cu, Zn by plasma emission spectroscopy; a subset of these samples has been analysed for REE, Th, Ta and Hf by INAA at the Institute of High Energy Physics in Beijing. The location of these samples is available from Deng Wanming on request. Microprobe analyses of clinopyroxenes and spinels in the basic and ultrabasic rocks from the Banggong Suture were carried out at the Institute of Geology in Beijing.

The four ophiolite belts are now considered in turn.

PHILOSOPHICAL TRANSACTIONS OF THE ROYAL SOCIETY A MATHEMATICAL, PHYSICAL & ENGINEERING SCIENCES

3. Yarlung–Zangbo ophiolite belt

(*a*) *Geology*

The Yarlung–Zangbo ophiolite belt extends from Ladakh in the west, where it connects with the Indus ophiolite belt, to the bend in the Zangbo river in the east and then extends discontinuously southwards along the Naga hills (figures 1 and 2). It is bordered in the north by the Ladakh and Gangdese granitoid belt and in the south by the low-grade metamorphics of the Himalayan Series over which the ophiolite fragments have been thrust southwards. The age of formation of the ophiolite has been dated as Albian (approximately 110 Ma) from radiolaria in interbedded cherts (Marcoux *et al.* 1982), and at 120 ± 10 Ma using Pb isotopes in clinopyroxenes from peridotites and dolerites (Göpel *et al.* 1984). The ophiolite is unconformably overlain by Xigaze Group flysch, the base of which has been dated using orbitolines as Aptian–Albian (Cherchi & Schroeder 1980), and was probably obducted during the Eocene (e.g. Molnar & Tapponnier 1975).

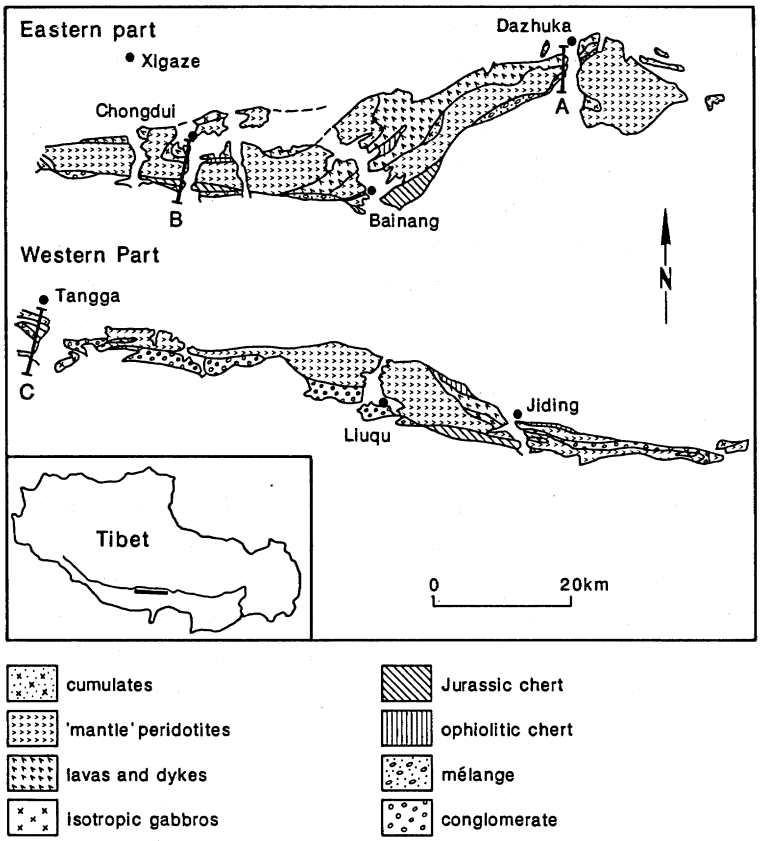

Figure 2. Map of the Yarlung–Zangbo ophiolite in the region studied during the Lhasa–Kathmandu 1986 traverse.

The part of the ophiolite belt studied briefly by us during the 1986 traverse from Lhasa to Kathmandu is shown in figure 2. It can be considered in two parts: an eastern part south of Xigaze between Chongdui and Dazhuka; and a western part north of Lhaze between Tangga and Liuqu. Sections through the ophiolite at Dazhuka, Chongdui and Tangga are shown in figure 3 and schematic reconstructions of the ophiolite in these areas, and at Jiding, are shown in figure 4.

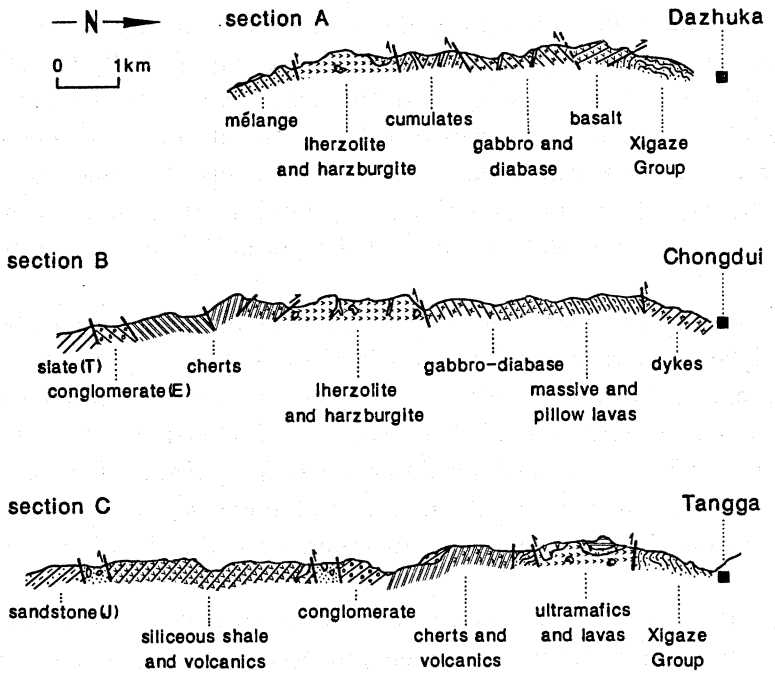

FIGURE 3. Geological sections through the Yarlung–Zangbo ophiolite. Locations of sections are shown in figure 2.

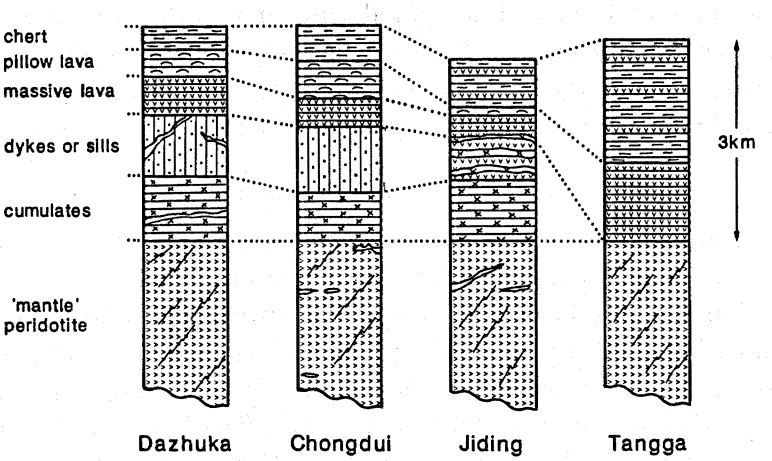

FIGURE 4. Schematic reconstructions of the Yarlung–Zangbo ophiolite for the sections shown in figure 3 and for a section just west of Jiding.

The tectonized ultramafic unit typically comprises about 1 km of serpentinized dunites and harzburgites which grade downwards into a further kilometre of fresh harzburgite with dunite patches and then into a maximum 4 km of exposure of fresh harzburgite containing 1–3% chrome diopside (e.g. Deng 1981, 1982, 1983, 1984; Girardeau *et al.* 1985*b*). Lherzolites are locally present, especially at the base of the unit, and also form the strongly serpentinized Liuqu Massif. The uppermost part is usually invaded by a variable but often large (up to 50% by volume) proportion of dykes and inclined sheets of doleritic to microgabbroic texture; a small number of these intrusions is also found in the lower part of the ultrabasic unit. Structural and petrologic analyses of the tectonite unit has indicated relatively low temperatures of equilibration and deformation (*ca.* 1150 °C) (Nicolas *et al.* 1981; Girardeau *et al.* 1985*a*). It is also apparent that some dykes were intruded before deformation, some after deformation and serpentinization.

Of the sections studied, the cumulate mafic–ultramafic sequence is best exposed south of Dazhuka as an approximately 500 m-thick body of rhythmically-layered dunites, rare wehrlites, troctolites, anorthosites and gabbros; here as elsewhere the layered sequence grades into isotropic gabbros, at the top of which are metre-sized pockets of plagiogranite. These gabbros are also cut by numerous dykes and inclined sheets. The thickest layered sequence reported from the area (2.5 km of continuous section) is at Angren, northwest of Lhaze (Prinzhofer *et al.* 1984). The total thickness of the plutonic unit appears to be on average about 3 km.

Sheeted dyke swarms are rare in the Xigaze–Lhaze area, but occur locally, for example at Baining, where dykes of average width 1.7 m strike E/W–ENE/WNW and dip south at a steep angle. More commonly, isotropic gabbros are overlain by massive and pillowed lavas and the whole sequence is subsequently intruded by dykes and inclined sheets. In the Dazhuka and Chongdui sections, mafic massive lavas or sills are overlain by mafic pillow lavas. The diameter of individual pillows is on average about 1 m and the lavas are often vesicular. In the Lhaze–Tangga sections sheeted lavas or sills are found intercalated with, or intruding, siliceous sediment.

A number of authors (e.g. Nicolas *et al.* 1981; Girardeau *et al.* 1985*a*, *b*) have reconstructed the Xigaze ophiolite and noted that, even taking into account the lack of continuity of exposure, the crustal section appears to be thin (approximately 3–3.5 km) compared with an off-axis oceanic crustal average of 7 km and compared with many other well-preserved ophiolites. Furthermore, the general absence of a sheeted dyke complex between the gabbros and pillow lavas, together with an abundance of dykes, sills and sill swarms throughout the section indicates an unusual type of crust, related, the above authors suggest, to a very slow-spreading ridge axis.

(*b*) *Petrology and geochemistry*

The bulk of our work on the geochemistry of the Xigaze ophiolite is applied to the dykes, sills and pillow lavas. Representative analyses are given in table 1.

Some typical analyses have been plotted as MORB-normalized multi-element patterns and chondrite-normalized rare earth patterns in figure 5. The MORB-normalized patterns are flat for the pillow lavas, massive lavas and dykes, indicating a N-type MORB composition and this is confirmed by the LREE-depleted rare earth patterns. The sills within the siliceous sediments, by contrast, have MORB-normalized patterns characterized by selective enrichment in the more incompatible elements, and REE-patterns that show LREE enrichment. The Ti–Zr–Y diagram (figure 6*a*) shows that this enrichment is sufficient to place the two analysed samples of sills on the boundary between the ocean ridge and within-plate basalt fields (c.f. figure 3 of Pearce & Mei, this volume). It is also apparent from table 1 that these enriched rocks also contain high concentrations of Ti and Fe and could be classed as FeTi basalts. The latter feature is commonly associated with high level magma chambers in propagating rifts. Other samples form a very tight cluster on the Ti–Zr–Y diagram indicative of a uniform magma type of MORB or volcanic arc basalt character: the Cr–Y discriminant diagram (figure 6*b*) then demonstrates that they are of MORB composition.

(*c*) *Tectonic interpretation*

The data presented here thus confirm the general consensus that the Yarlung–Zangbo ophiolite in the Xigaze region is predominantly of N-MORB composition. Although such compositions can be found in incipient oceans or back-arc basins, an absence of clastic sediments

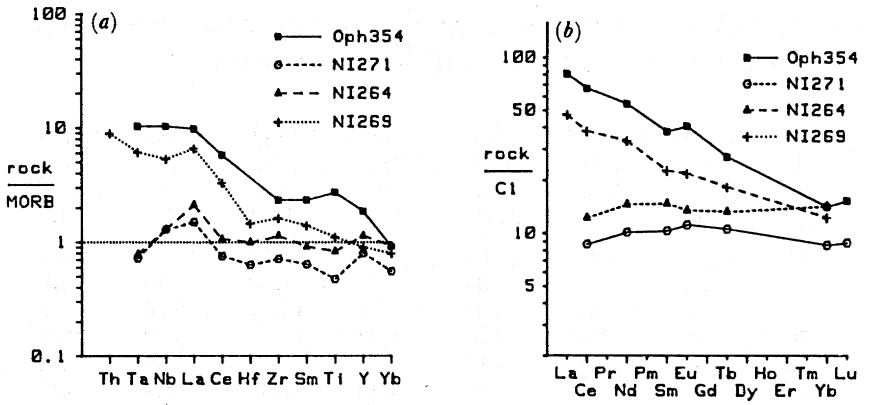

FIGURE 5. (*a*) MORB-normalized trace element patterns and (*b*) chondrite-normalized rare-earth patterns for lavas and dykes from the Yarlung–Zangbo ophiolite. For full analyses and sample localities, see table 1.

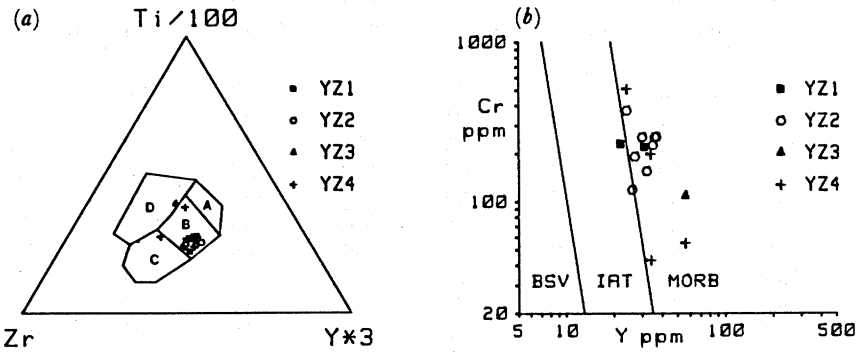

FIGURE 6. (*a*) Ti–Zr–Y and (*b*) Cr–Y discriminant diagrams for lavas and dykes from the Yarlung–Zangbo ophiolite. In figure 6*a*, within-plate field basalts plot in field D, calc-alkaline basalts in fields B and C, mid-ocean ridge basalts in field B and island arc tholeiites in fields A and B. In figure 6*b*, mid-ocean ridge basalts, island arc tholeiites and boninite series volcanics plot in the MORB, IAT and BSV fields respectively. Key to localities: YZ1 = Dazhuka; YZ2 = Chongdui; YZ3 = Jiding; YZ4 = Tangga. The two points plotting on the field B–D boundary in figure 6*a* and towards higher Y values in figure 6*b* are sills.

and, in the latter case also an absence of lavas of arc composition, suggests that the setting was genuinely intraoceanic. The composition of the sills within the overlying siliceous sediment also supports this interpretation, their intraplate composition being consistent with off-axis magmatism in a major ocean.

Nicolas *et al.* (1981) and Girardeau *et al.* (1985*a*, *b*) argue that the thin crustal structure and complex intrusive patterns, as shown by the sill complexes, are indications that the ophiolite formed at a very slow spreading ridge. Pozzi *et al.* (1984) demonstrated that this ridge was oriented approximately north–south and suggested that the ophiolite fragments represented small spreading segments offset by major transforms. They rejected, however, the hypothesis of Sengör (1981) that the transforms had a major part to play in the origin of the ophiolite.

The view of the Lhasa–Kathmandu Geotraverse team, notably Kidd, Abbate and Xenophontos (pers. comms), and supported by ourselves, is that the ophiolites do show major evidence of generation at or near ridge-transform intersections. The main lines of evidence are as follows.

(1) Evidence from extant ocean basins suggests that the degree of partial melting of the

Table 1. Representative geochemical analyses for selected samples of lavas and dykes from the Yarlung-Zangbo ophiolite belt

sample	Oph302	Oph303	Oph163	NI475	NI462	NI463	NI319	NI458	NI324
location	YZ1	YZ1	YZ1	YZ2	YZ2	YZ2	YZ2	YZ2	YZ2
rock	bas.	bas.	bas.	bas.	bas.	bas.	bas.	bas.	bas.
type	PL	ML	D	PL/C	PL/C	PL/C	PL	PL	PL
SiO_2	47.61	52.99	51.93	47.30	54.30	54.00	44.60	48.20	55.10
TiO_2	.98	.61	.71	.93	.98	1.15	1.30	1.10	1.18
Al_2O_3	17.89	17.08	15.26	15.90	16.30	16.40	12.90	14.70	14.20
Fe_2O_3	9.76	7.02	8.97	9.70	8.33	10.50	9.20	9.31	9.63
MnO	.18	.14	.14	.11	.12	.09	.30	.16	.14
MgO	5.25	6.10	7.42	5.80	4.43	4.67	9.24	5.51	5.99
CaO	9.51	6.58	6.70	12.20	6.68	4.09	14.70	11.00	7.09
Na_2O	3.65	4.80	5.16	4.04	5.21	7.15	1.20	3.70	4.34
K_2O	.55	.30	.16	.12	1.25	.50	.02	.80	.46
P_2O_5	.15	.06	.16	0.00	0.00	0.00	0.00	0.00	0.00
LOI	4.96	4.64	3.46	3.73	1.47	1.93	2.97	5.78	2.63
Total	100.49	100.07	100.07	99.83	99.07	100.48	96.43	100.26	100.76
Zr	98	63	0	60	67	82	93	94	107
Y	31	22	0	24	25	24	30	29	28
Nb	0.0	0.0	0.0	1.5	2.0	2.2	3.2	2.2	2.3
Rb	0.0	0.0	0.0	1.7	19.1	4.9	.5	15.1	6.0
Sr	180	165	0	92	288	122	29	120	128
Cr	220	230	0	252	191	155	253	253	225
Ni	81	130	0	65	55	56	76	81	77
V	230	140	0	224	166	181	273	224	206
Cu	68	13	0	35	20	15	59	31	21
Zn	0	0	0	72	74	70	93	84	83
Hf	0.00	0.00	0.00	1.54	1.79	1.97	2.36	2.50	2.42
Ta	0.00	0.00	0.00	0.00	.06	.09	.10	.09	.12
Th	0.00	0.00	0.00	0.00	0.00	0.00	0.00	0.00	0.00
Sc	0.0	0.0	0.0	32.8	30.9	31.4	32.9	27.8	28.7
Co	0.0	0.0	0.0	30.0	28.1	28.4	36.7	32.0	31.3
La	0.0	0.0	1.4	0.0	0.0	0.0	0.0	0.0	0.0
Ce	0.0	0.0	5.6	7.5	7.7	8.7	7.6	9.4	9.4
Nd	0.0	0.0	0.0	0.0	7.3	11.5	12.0	10.9	10.2
Sm	0.00	0.00	1.53	2.40	2.40	2.50	3.10	3.10	3.20
Eu	0.00	0.00	.66	.93	.93	.93	1.40	1.10	1.12
Tb	0.00	0.00	.45	.58	.62	.55	.80	.83	.73
Ho	0.00	0.00	0.00	0.00	0.00	0.00	0.00	0.00	0.00
Tm	0.00	0.00	.33	.41	.41	.45	.51	.48	.47
Yb	0.00	0.00	1.72	2.55	2.40	2.30	3.30	2.81	2.98
Lu	0.00	0.00	.26	.45	0.00	0.00	.50	.50	0.00

mantle, and hence the oceanic crustal thickness, decreases within ridge segments towards ridge-transform intersections; this would thus explain the thin crustal section (Fox & Straup 1981).

(2) Intraoceanic melanges with serpentinite matrices are important in oceanic fracture zones and are common in the Xigaze ophiolite, notably at Xiatu, where rodingitized gabbro and diabase blocks are found within a serpentinite matrix.

(3) Intraoceanic unconformities, in which coarse-grained clastic and pelagic sediments ovelie peridotites, are important in oceanic transform faults. They are also found in the Xigaze

TABLE 1. (*cont.*)

sample	Oph174	Oph171	Oph351	Oph93	Oph354	NI271	NI264	NI269	L-20
location	YZ2	YZ2	YZ2	YZ3	YZ3	YZ4	YZ4	YZ4	YZ4
rock	bas.	bas.	bas.	bas.	bas.	bas.	bas.	bas.	bas.
type	PL	ML	D	ML	S	ML?	ML?	S?	S
SiO_2	49.32	47.93	55.02	47.95	46.99	51.80	50.50	42.20	49.03
TiO_2	.84	.90	.76	.74	4.08	.71	1.24	1.66	3.52
Al_2O_3	15.26	15.05	14.77	14.23	12.86	12.90	15.90	15.20	12.63
Fe_2O_3	8.99	8.32	8.98	9.44	16.83	9.20	10.40	9.87	15.87
MnO	.15	.16	.20	.22	.29	.17	.15	.17	.32
MgO	7.94	6.60	7.11	8.04	4.98	8.45	5.86	5.75	3.81
CaO	6.99	5.68	4.87	11.80	7.80	11.10	7.80	20.20	8.03
Na_2O	5.13	5.00	3.70	.40	3.65	2.95	4.04	4.02	4.40
K_2O	.23	.10	.55	.10	.40	.84	.12	.76	.16
P_2O_5	.16	.19	.06	.09	.21	0.00	0.00	0.00	.32
LOI	5.42	10.51	4.35	7.37	2.45	1.14	3.73	3.73	2.85
Total	100.43	100.44	100.37	100.38	100.54	99.26	99.74	103.56	100.94
Zr	61	66	0	0	210	64	102	146	173
Y	24	26	0	0	56	24	34	27	56
Nb	0.0	0.0	0.0	0.0	0.0	4.0	4.0	16.5	0.0
Rb	0.0	0.0	0.0	0.0	0.0	4.0	12.0	2.7	0.0
Sr	128	54	0	0	42	229	139	928	180
Cr	372	118	0	0	108	511	43	199	55
Ni	84	52	0	0	90	136	47	142	60
V	170	200	0	0	420	193	249	245	419
Cu	36	19	0	0	254	12	38	37	170
Zn	0	0	0	0	0	81	87	83	0
Hf	0.00	0.00	0.00	0.00	0.00	1.51	2.38	3.48	0.00
Ta	0.00	0.00	0.00	0.00	0.00	.13	.14	1.10	0.00
Th	0.00	0.00	0.00	0.00	0.00	0.00	0.00	1.79	0.00
Sc	0.0	0.0	0.0	0.0	0.0	36.8	27.8	25.7	0.0
Co	0.0	0.0	0.0	0.0	0.0	38.8	33.7	35.9	0.0
La	1.1	1.4	2.3	0.0	26.4	0.0	0.0	15.5	0.0
Ce	4.3	4.7	7.8	0.0	57.7	7.5	10.6	32.9	0.0
Nd	0.0	0.0	0.0	0.0	34.3	6.4	9.2	21.1	0.0
Sm	1.56	1.79	1.88	0.00	7.69	2.10	3.00	4.60	0.00
Eu	.76	.65	1.04	0.00	3.13	.86	1.04	1.68	0.00
Tb	.54	.58	.55	0.00	1.41	.55	.69	.95	0.00
Ho	0.00	0.00	0.00	0.00	0.00	0.00	0.00	0.00	0.00
Tm	.37	.38	.39	0.00	0.00	0.00	.54	.48	0.00
Yb	1.87	2.29	2.45	0.00	3.11	1.88	3.14	2.70	0.00
Lu	.28	.38	.41	0.00	.52	.30	0.00	0.00	0.00

Elements Si to Zn were analysed by XRF and AA, elements Hf to Lu by INAA. Non-detected/unanalysed elements given as 0. Key to locations: YZ1 = Dazhuka; YZ2 = Chongdui; YZ3 = Jiding; YZ4 = Tangga. Key to rock types: bas. = basalt; PL = pillow lava; ML = massive lava; C = conglomerate; D = dyke.

ophiolite, for example between Gyangze and Xigaze (2907N 8900E) where sheared harzburgite was seen to be overlain by some 2.5 m of ophicalcite breccia, then 30 m of chert-rich clastics and finally > 50 m of red cherts.

(4) Intrusion of dykes into 'cold' oceanic lithosphere, common in the Xigaze ophiolite, is likely to be restricted to ridge-transform intersections where lateral propagation of dykes can take place from the active ridge segment into newly formed lithosphere. Moreover the intrusion of dykes into serpentinized peridotite requires an environment for serpentinization soon after formation that is best provided by a transform zone.

PHILOSOPHICAL TRANSACTIONS OF THE ROYAL SOCIETY A MATHEMATICAL, PHYSICAL & ENGINEERING SCIENCES

(5) Transform faults are likely sites of the off-axis volcanism seen as sills or flows within overlying sediments.

(6) The lower degree of partial melting in transform zones means that the residual peridotites will be less depleted than beneath the central parts of ridge segments (Ishiwatari 1985); lherzolites such as those from the Liuqu massif are thus likely to be typical of intrusions within transform zones.

Thus, although we agree with the general setting of the ophiolite as proposed by Pozzi *et al.* (1984) and illustrated in figure 7, we consider the character of the ophiolite to relate as much or more to transform faults than to a slow spreading environment.

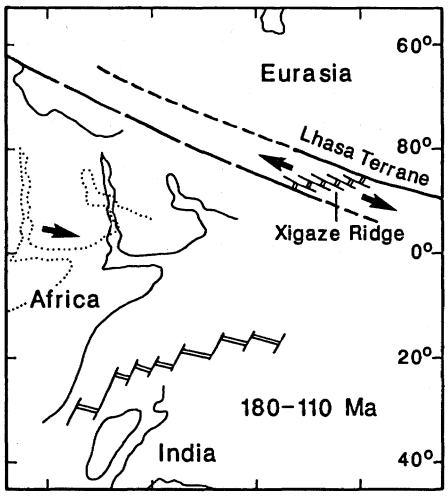

FIGURE 7. Model of Pozzi *et al.* (1984) for the tectonic environment of formation of the Yarlung–Zangbo ophiolite.

4. BANGGONG LAKE–NUJIANG RIVER OPHIOLITE BELT

(*a*) *Geology*

The ophiolite belt associated with the Banggong Suture zone is well exposed in the geotraverse section between the villages of Nagqu, Amdo, Dongqiao and Gyanco (figures 1 and 8), where it has been termed the Dongqiao ophiolite by Girardeau *et al.* (1985*c*). The ophiolite belt is dispersed over a north–south distance of some 200 km and can be divided into several subzones which are roughly parallel to one another (figure 8). This study involved the field examination and sampling of a number of localities within these zones; these localities are shown in figure 8 and the ophiolitic units exposed shown in schematic section in figure 9.

The southernmost subzone (Zone IV), which contains the Xainxa ultramafic rocks described by Girardeau *et al.* (1985*c*), was not visited during the geotraverse, although one of us (Deng) has worked in the area. The Zone contains thin slices dominantly of harzburgite with minor dunite bodies and rare podiform chromites (e.g. at Yangzhong); mafic rocks in the form of isotropic gabbro clasts in serpentinite have been reported from one locality in the Nychang area. These slices are thought to represent southward-thrust klippen from a suture to the north.

The next zone (Zone III) includes the ophiotitic bodies at Baila and Ado west of Gyanco, Nalong east of Gyanco and the Yila Massif northwest of Nagqu. Tectonized ultramafics were

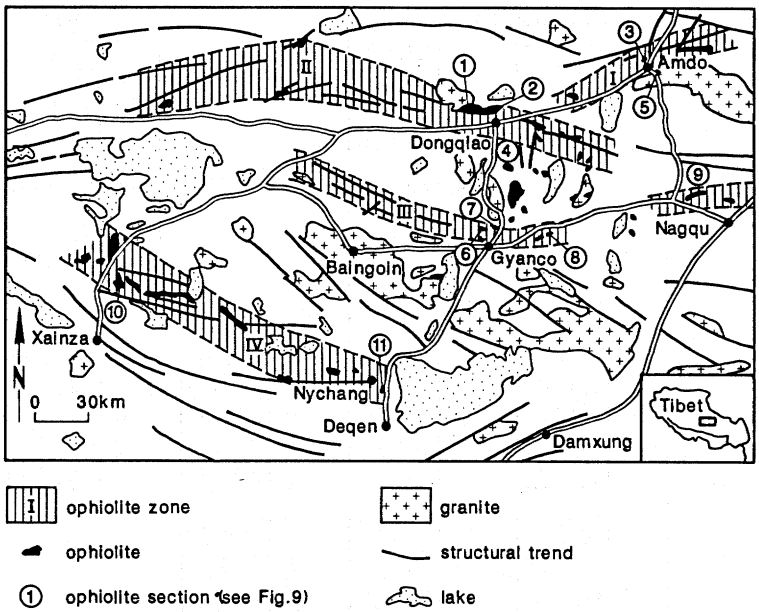

FIGURE 8. Geological setting of the Banggong Lake–Nujiang River ophiolite belt and locations of the areas discussed in the text and represented in figure 9.

studied in the Ado, Nalung and Yila Massifs where they mostly occur as harzburgites with minor dunites, although lherzolites have been sampled in the Ado Massif; they are cut in the Ado Massif west of Pung Co by rodingitised microgabbro dykes. Layered plutonic sections, examined in the Baila and Yila Massifs, comprise dunite–wehrlite sections overlain by layered gabbros. The Ado massif does, however, contain a small troctolite–gabbro body. A small dyke complex cut by dioritic dykes, previously described in detail by Girardeau *et al.* (1984), was studied and sampled in the Baila massif. Lavas are represented mainly in a section some 100 m thick at Nalung, where generally massive flows are overlain by pillowed flows, all cut at a high angle by a series of thin, isolated diabase dykes.

Zone II was studied around Dongqiao, where the major exposures are of harzburgites with minor dunite–chromite bodies and including one significant podiform chromite deposit. Northwest of Donqiao, the harzburgite is in thrust contact with an overturned amphibolitized sequence comprising pillow lavas overlain by pelagic sediments. South of Donqiao, at Loubochong, is an inverted pillow lava sequence described by Pearce & Mei (this volume). As stated in that paper, it is not clear whether or not these lavas belonged to an ophiolite complex or to some non-ophiolitic submarine volcanic edifice.

Zone I was studied south of Amdo village where ophiolites crop out east and west of the main highway. The rock types here range from a sheeted dyke complex comprising 100% dykes through an area of mainly dykes with pillow screens into 100% pillow lavas. In fault contact with this complex is the sequence of lavas of island arc composition described by Pearce & Mei (this volume).

The age of formation of the ophiolite has been identified as Jurassic from isotopic dating of late-magmatic amphiboles (Maluski, Girardeau & Tang, pers. comm. 1986) and by biostratigraphic dating of radiolaria in interbedded cherts (Tang & Wang 1984). Obduction of the ophiolite had taken place by the end of the Jurassic, as indicated by shallow water to

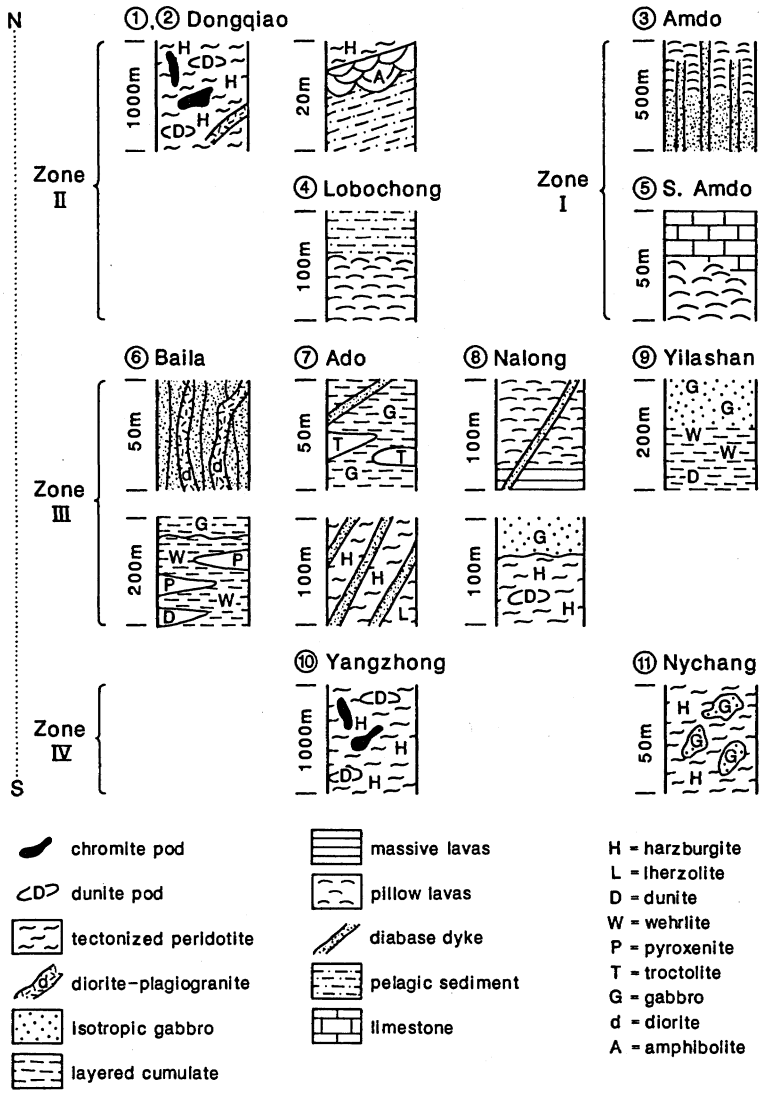

FIGURE 9. Schematic geological sections from some of the studied areas from the Banggong Lake–Nujiang River ophiolite belt. For locations, see figure 8.

continental deposits of the overlying Zigetang formation which have a latest Jurassic to earliest Cretaceous age (Girardeau *et al.* 1985*c*). Mid-Cretaceous redbeds and volcanics unconformably overlie the ophiolite and its sedimentary cover and are thought to post-date the final collision.

Because of the highly fragmentary nature of the ophiolite, the structure has been pieced together from outcrops that expose different levels of the complex (Girardeau 1985*c*). While necessary to obtain a stratigraphy, this approach does assume that (*a*) all fragments belonged to the *same* oceanic lithosphere and (*b*) all fragments belonged to oceanic lithosphere rather than other intraoceanic features. This study aims to use geochemical characterization techniques to evaluate these hypotheses and to consider in further detail the original environment of formation.

(*b*) *Petrology and geochemistry*

Evidence relating to the original tectonic setting of the ophiolite has been obtained from all parts of the complex. Spinel analyses from the tectonized ultramafic units have been plotted on the diagram of Dick & Bullen (1984) in figure 10, and some representative data are given in table 3. It is apparent from figure 10 that the data fall into two groups: the main group is characterized by the harzburgite-hosted spinels which have high Cr# (Cr/(Cr+Al) ratios) and plot in the boninite and island arc basalt fields on the diagram; a second group, restricted to the Ado locality, is characterized by lherzolite-hosted spinels which have low Cr# and plot in the abyssal peridotite field. Spinels from cumulate dunites have also been plotted on this diagram and reinforce the bimodality of composition. Following the petrogenetic arguments of Dick & Bullen (1984), the harzburgite-hosted high-Cr# spinels are likely to represent residua from a high degree of melting (or re-melting) of the mantle, an interpretation supported by the refractory clinopyroxene-free (15–25 % opx, 70–85 % ol, < 1 % sp) and low Al_2O_3 (0.2–1.5 %) character of their host rocks and indicative of a supra-subduction zone origin. The lherzolite-hosted spinels from the Ado Massif are likely to have been derived by the lower degrees of melting or less depleted sources that characterize MORB genesis.

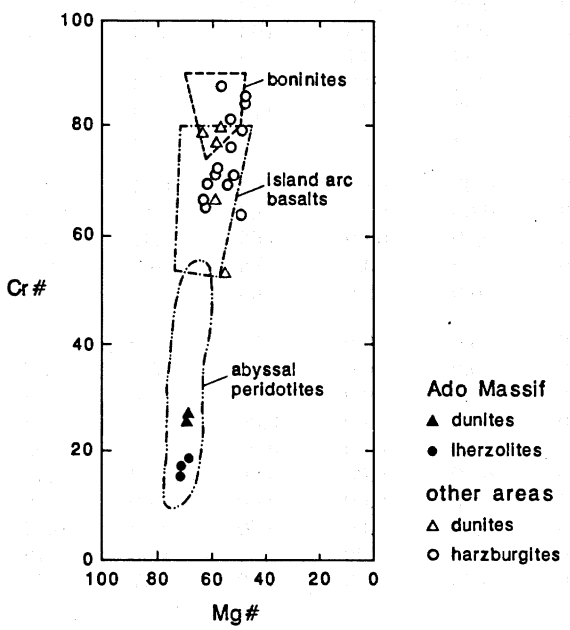

FIGURE 10. Chrome spinel compositions from dunites and tectonized ultramafic rocks from the Banggong Lake–Nujiang River ophiolite belt plotted on the Cr#–Mg# diagram of Dick & Bullen (1984). For representative full analyses, see table 3.

The crystallization sequence of the cumulates also supports a supra-subduction zone origin for almost all the plutonic sequences studied, showing an olivine–clinopyroxene–plagioclase order of crystallization resulting in dunite–wehrlite sequences. Parts of the Ado Massif again present an exception, indicating an olivine–plagioclase–clinopyroxene order of crystallization resulting in a dunite–troctolite sequence. Although crystal cumulation generally prevents the use of whole-rock geochemistry for characterization of these rocks, the Baila diorite is sufficiently

TABLE 2. REPRESENTATIVE GEOCHEMICAL ANALYSES FOR SELECTED SAMPLES OF LAVAS AND DYKES FROM THE BANGGONG SUTURE ZONE OPHIOLITE BELT

sample	G95C	G95B	G95D	G95F	Oph404	1-8	1-8	G92F	Lang-2
location	BG1	BG1	BG1	BG1	BG2	BG2	BG2	BG2	BG2
rock	bon.	bon.	bon.	bas.	b/a.	b/a.	b/a.	bas.	b/a.
type	D	D	D	D	PL	PL	PL	D	D
SiO_2	61.20	51.00	49.10	45.30	53.13	54.20	53.44	51.80	52.59
TiO_2	.41	.50	.32	.40	.58	.51	.52	.59	.81
Al_2O_3	10.60	12.70	16.40	18.40	13.58	13.40	13.68	15.20	14.90
Fe_2O_3	6.23	8.48	9.28	11.28	9.65	9.48	9.44	7.76	9.60
MnO	.12	.14	.12	.11	.18	.19	.18	.14	.18
MgO	10.50	14.60	7.50	6.58	6.89	9.56	9.53	6.52	6.84
CaO	5.69	6.48	10.64	11.10	8.32	7.19	7.89	15.00	6.98
Na_2O	3.49	3.42	1.86	1.22	4.55	4.14	3.95	.98	4.49
K_2O	.06	.06	1.14	1.54	.60	.17	.33	.12	.66
P_2O_5	.11	.15	.02	.04	.08	.06	.04	.05	.08
LOI	1.76	2.47	3.80	3.72	2.26	1.58	1.52	1.70	3.65
Total	100.17	100.00	100.18	99.69	99.82	100.48	100.52	99.86	100.78
Zr	56	67	15	54	0	0	0	34	0
Y	8	10	9	28	0	0	0	14	0
Nb	2.8	3.6	3.3	5.1	0.0	0.0	0.0	1.8	0.0
Rb	1.0	0.0	16.3	8.0	0.0	0.0	0.0	1.5	0.0
Sr	90	150	228	532	0	0	0	214	0
Cr	540	634	56	103	220	404	385	360	198
Ni	203	258	41	49	85	157	141	87	94
V	130	200	338	573	200	0	0	250	325
Cu	108	25	348	478	0	0	0	20	0
Zn	60	85	57	57	0	0	0	54	0
Hf	0.00	0.00	0.00	0.00	1.04	0.00	0.00	1.00	0.00
Ta	0.00	0.00	0.00	0.00	.14	0.00	0.00	.13	0.00
Th	0.00	0.00	0.00	0.00	.37	0.00	0.00	.30	0.00
Sc	0.0	0.0	0.0	0.0	0.0	0.0	0.0	36.8	0.0
Co	0.0	0.0	0.0	0.0	0.0	0.0	0.0	35.4	0.0
La	0.0	0.0	0.0	0.0	2.0	2.1	2.1	1.6	3.9
Ce	0.0	0.0	0.0	0.0	5.3	4.8	5.1	5.6	9.1
Nd	0.0	0.0	0.0	0.0	0.0	3.8	0.0	3.9	9.3
Sm	0.00	0.00	0.00	0.00	1.37	1.25	1.32	1.41	2.18
Eu	0.00	0.00	0.00	0.00	.50	.55	.59	.69	.63
Tb	0.00	0.00	0.00	0.00	.42	.40	.39	.39	.74
Ho	0.00	0.00	0.00	0.00	0.00	0.00	0.00	0.00	0.00
Tm	0.00	0.00	0.00	0.00	0.00	0.00	0.00	.20	0.00
Yb	0.00	0.00	0.00	0.00	1.68	1.70	1.84	1.53	2.53
Lu	0.00	0.00	0.00	0.00	.27	.28	.31	.26	.38

homogeneous to be used in this way: its composition, shown in table 2, shows low incompatible element content and a slight LREE enrichment (figure 11) typical of intermediate rocks of the island arc tholeiite series.

Geochemical discriminants applied to the lavas and dykes further support these broad conclusions, but also provide more detail on the type of supra-subduction zone environment. The diagrams used, MORB-normalized trace element patterns, rare-earth element patterns and Th–Ta–Hf+Cr–Y discriminant plots are shown in figures 12 and 13 respectively. Data representative of those on which these diagrams are based are listed in table 2.

Figure 12 shows patterns representative of Nalong (G92F), Loubochong (G106D), Dongqiao amphibolite (G103C) and Amdo (G127C) pillow lavas. It will be noted that all patterns show

TABLE 2. (*cont.*)

sample	Oph450	G106D	G103C	G127C	Amdo-1	Amdo-5	Oph622	Amdo10	G106D
location	BG3	BG3	BG4	BG5	BG5	BG5	BG5	BG5	BG6
rock	bas.	bas.	bas.	bas.	bas.	bas.	bas.	b/a.	bas.
type	PL	PL	PL	D?	D	D	D?	D?	PL
SiO_2	51.35	47.60	49.80	50.30	48.75	49.59	48.99	53.28	47.60
TiO_2	0.64	0.56	1.22	1.24	.69	1.43	1.22	1.42	.56
Al_2O_3	13.32	11.20	12.80	14.20	13.94	12.90	13.75	12.02	11.20
Fe_2O_3	9.84	6.20	9.36	12.20	10.85	14.98	13.33	13.08	6.20
MnO	0.38	0.15	.17	.19	.15	.29	.21	.20	.15
MgO	3.78	5.04	7.78	7.30	8.24	6.60	7.53	6.37	5.04
CaO	7.35	15.90	13.50	9.95	11.60	7.91	8.42	7.47	15.90
Na_2O	4.90	3.51	3.34	2.71	2.06	3.20	3.34	3.93	3.51
K_2O	0.25	0.68	.28	.22	.11	.10	.05	.05	.68
P_2O_5	0.12	0.09	.10	.08	.05	.09	.07	.12	.09
LOI	7.06	9.98	2.22	1.43	3.80	3.51	4.10	3.20	9.98
Total	98.99	100.91	100.57	99.82	100.24	100.60	101.01	101.14	100.91
Zr	0	32	68	60	0	0	0	0	32
Y	0	11	23	30	0	0	0	0	11
Nb	0.0	2.4	4.0	2.0	0.0	0.0	0.0	0.0	2.4
Rb	0.0	13.0	6.4	3.5	0.0	0.0	0.0	0.0	13.0
Sr	0	157	199	96	0	0	0	0	157
Cr	0	480	200	107	278	59	250	51	480
Ni	0	217	65	47	90	46	130	56	217
V	0	180	290	340	316	456	320	420	180
Cu	0	35	122	55	0	0	0	0	35
Zn	0	51	132	99	0	0	0	0	51
Hf	1.38	.91	1.80	1.75	0.00	0.00	0.00	0.00	.91
Ta	.14	.11	.26	.12	0.00	0.00	0.00	0.00	.11
Th	.72	.69	.73	.30	0.00	0.00	0.00	0.00	.69
Sc	0.0	27.1	37.5	29.4	0.0	0.0	0.0	0.0	27.1
Co	0.0	34.8	38.0	48.9	0.0	0.0	0.0	0.0	34.8
La	6.6	3.6	3.4	1.5	1.7	2.9	3.1	3.2	3.6
Ce	11.2	9.5	10.0	6.8	5.1	9.4	8.3	7.7	9.5
Nd	6.4	5.8	7.8	7.7	0.0	11.9	0.0	8.6	5.8
Sm	1.86	1.50	2.61	3.00	1.89	3.75	2.68	3.64	1.50
Eu	.70	.52	.97	1.00	.85	1.42	1.10	1.41	.52
Tb	.44	.36	.73	.87	.42	1.21	.74	1.10	.36
Ho	0.00	1.00	1.80	0.00	0.00	0.00	0.00	0.00	1.00
Tm	0.00	.16	.25	0.00	0.00	0.00	0.00	0.00	.16
Yb	1.65	1.33	2.76	3.61	2.57	4.41	3.21	4.90	1.33
Lu	.26	.23	.42	.59	.36	.69	.53	.67	.23

Elements Si to Zn were analysed by XRF and AA, elements Hf to Lu by INAA. Non-detected/unanalysed elements given as 0. Key to locations; BG1 = Baila; BG2 = Nalong; BG3 = Loubochong; BG4 = Dongqiao; BG5 = Amdo; BG6 = Amdo (S). Key to rock types: bas. = basalt; b./a. = basaltic andesite; PL = pillow lava; D = dyke; bon. = boninite; dior. = diorite; L = massive lava.

an enrichment in Th relative to Ta indicative of a supra-subduction zone environment, although the twofold enrichment at Nalong is relatively small. In addition, the Loubochong sample shows the greatest subduction component with enrichment of LREE and P as well as Th and hence a more calc-alkaline composition. Variations are also apparent in figure 13: only the Loubochong pattern shows LREE enrichment; the Amdo sample exhibits strong LREE depletion; and the other two samples show slight depletion.

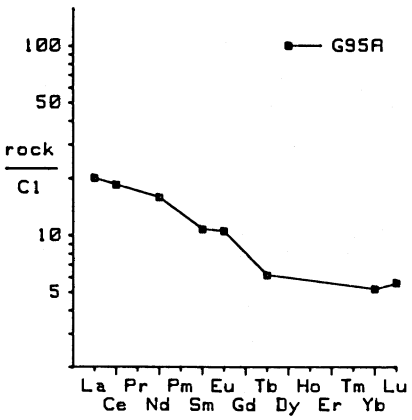

FIGURE 11. Chondrite-normalized rare-earth pattern for the diorite at Baila.

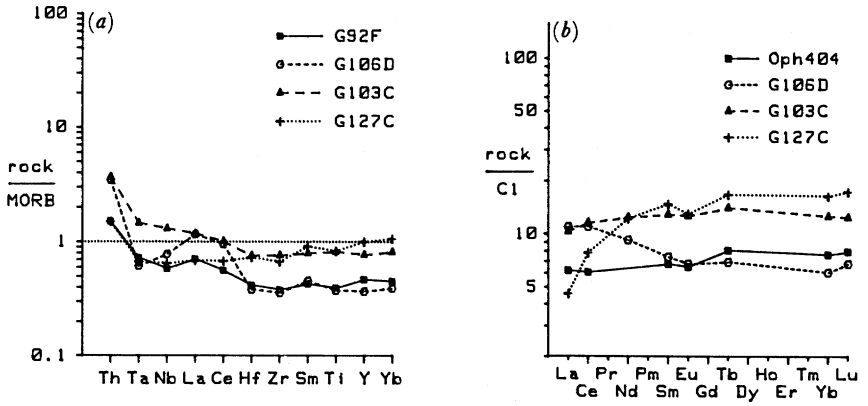

FIGURE 12. (*a*) MORB-normalized trace element patterns and (*b*) chondrite-normalized rare earth patterns for representative samples from the Banggong Lake–Nujiang River ophiolite belt. For full analyses and sample localities, see table 2.

TABLE 3. REPRESENTATIVE MINERAL ANALYSES FROM ULTRABASIC AND BASALTIC ROCKS FROM THE BANGGONG–NUJIANG OPHIOLITE BELT

sample	Nych.	Dong.	Nych.	Ado	Ado	Ado	Ado	Amdo	Nalong
location	OPH546	OPH459	OPH546	Ado-1	Ado-1	Ado-1	Ado-1	Amdo9	OPH403
rock	harz.	harz.	harz.	lherz.	lherz.	lherz.	lherz.	dol.	bas.
min.	ol.	opx.	sp.	ol.	opx.	cpx.	sp.	cpx.	cpx.
SiO_2	39.48	58.14	.06	41.16	54.90	50.54	.03	48.46	51.37
TiO_2	.05	0.00	.39	.05	.11	.31	0.00	.15	.31
Al_2O_3	0.00	.98	7.22	0.00	4.74	7.04	53.34	4.80	4.55
FeO	7.31	4.83	19.16	8.26	6.51	2.60	12.96	17.29	5.82
MnO	.12	.03	.33	.03	.12	.03	.21	.30	.18
MgO	51.67	34.72	9.46	47.21	32.27	15.16	18.55	13.06	17.92
CaO	.02	.73	.02	.04	.76	21.45	0.00	11.02	19.20
Na_2O	.02	.04	.02	.02	.05	.89	.02	.42	.17
Cr_2O_3	0.00	.39	59.31	.04	.50	.99	15.46	.07	.21
Total	98.67	99.86	95.97	96.81	99.96	99.01	100.57	95.57	99.73
Mg#	.93	.93	.47	.91	.90	.91	.71	.57	.84
Cr#	0.00	0.00	.85	0.00	0.00	0.00	.16	0.00	0.00

Key to locations: Nych. = Nychang; Dong. = Dongqiao. Key to rock types: harz. = harzburgite; lherz. = lherzolite, dol. = dolerite; bas. = basalt. Key to minerals: ol. = olivine; opx. = orthopyroxene; cpx. = clinopyroxene; sp. = spinel.

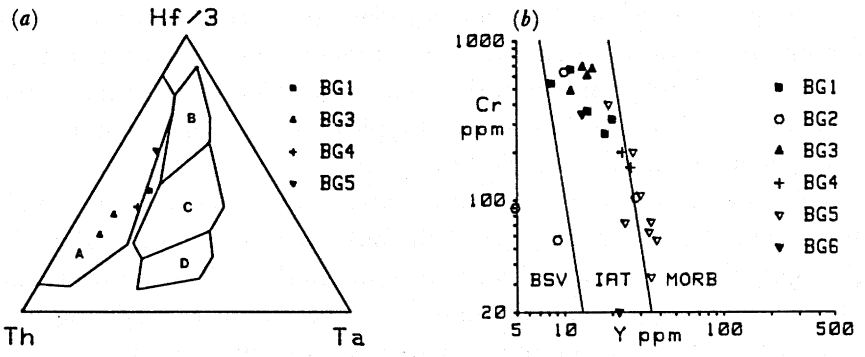

FIGURE 13. (*a*) Th–Ta–Hf and (*b*) Cr–Y discriminant diagrams for basic lavas from the Banggong Lake–Nujiang River ophiolite belt. In figure 13*a*, volcanic arc basalts plot in field A, mid-ocean ridge basalts in fields B and C and within plate basalts in fields C and D. The fields in figure 13*b* are given in the caption to figure 5*b*. Key to localities: BG1 = Baila dykes; BG2 = Nalong lavas and dykes; BG3 = Loubochong pillow lavas; BG4 = Dongqiao amphibolite; BG5 = Amdo pillow lavas/dykes; BG6 = S. Amdo lavas.

Figure 13*a* further demonstrates the selective enrichment of Th over Ta in these rocks which cause the compositions to be displaced away from the MORB field towards the field of volcanic arc basalts. Figure 13*b* shows a greater number of analyses and permits a more detailed discrimination between boninite series volcanics (BSV), island arc tholeiites (IAT) and mid-ocean ridge basalt (MORB) compositions. It is apparent that two of the dykes from Baila have very low Y and high Cr values and plot within the BSV field. This interpretation is supported by inspection of the major element compositions of these rocks in table 3 which, despite alteration, show the combination of high SiO_2 and high MgO that characterizes the BSV series. These compositions, and particularly the variable enrichment in Zr relative to Y, resemble those of the Arakapas area of the Troodos Massif of Cyprus (Rogers *et al*, in press). However it should also be noted that other dykes from this complex show more tholeiitic compositions. Also on this diagram, the lavas and dykes from Nalong span the IAT field, the lavas from Loubochong and South Amdo plot in the centre of the IAT field, and the Dongqiao amphibolite and the lavas and dykes from Amdo plot on the boundary between the MORB and IAT fields.

The primary mineralogy of the lavas and dykes also varies from south to north, although greenschist, sometimes zeolite or amphibolite, facies alteration has affected all rocks. The lavas and dykes in the southern and central zones are noticeably richer in clinopyroxene, sometimes containing clinopyroxene phenocrysts, than the more feldspar-rich lavas and dykes in the Amdo region. Microprobe analyses of clinopyroxenes (table 3) show a distinction between the more chrome-diopsidic compositions at Nalung and the more augitic compositions at Amdo; both groups of pyroxenes plot in orogenic, or island arc fields on pyroxene discrimination diagrams. The boninites are too altered for primary Ca-poor pyroxenes to be identified.

(*c*) *Tectonic interpretation*

The data presented here thus in general support the previous interpretations (Wang *et al.* 1984; Yang & Deng 1986; Girardeau *et al.* 1984) that the Dongqiao ophiolite formed in a supra-subduction zone setting. However, they also suggest that it may be too simplistic to construct a single ophiolite section from the isolated outcrops (Girardeau *et al.* 1984) since they have different compositions and therefore represent different types of oceanic lithosphere. It

may also be too simplistic to assume that all fragments represent klippen from a single suture since the compositional variety is equally, perhaps more, consistent with their emplacement during closure of an arc-basin complex rather than of a single basin. Finally, the lherzolites, troctolites and gabbros in the Ado Massif are of typical MORB composition and may represent incorporated fragments of normal oceanic lithosphere.

In the authors' opinion, the most significant observation is that of the regional zonation in the composition of the dykes and lavas. In their southernmost outcrops (Zone III), genuine boninitic high MgO, high SiO_2 compositions are found in the Baila dyke swarm and have also been reported from the Dengqen ophiolite in the same belt to the east (Zhang & Yang 1986); elsewhere in this belt (and also within the Baila dyke swarm) primitive island arc tholeiites are the normal magmatic product. Between this zone and the northern zones (I and II), typical island arc tholeiite series are present, some (those south of Amdo) clearly representing volcanic edifices rather than oceanic lithosphere (Pearce & Mei, this volume.) In the northern zones, transitional MORB–IAT compositions are found. This type of spatial zonation is common in Western Pacific island arcs, as for example from the Tonga fore-arc, through the Tofua arc to the Lau Basin and from the Mariana fore-arc through the Mariana arc to the Mariana trough (e.g. Hawkins & Melchior 1985; Dietrich *et al.* 1978). According to this analogy, the ophiolites from Zones III and IV would represent fore-arc lithosphere, the lavas from Loubochong and South Amdo would represent island arc and arc seamount edifices and the amphibolites of Zone II and lava-dyke complexes of Zone I would represent back-arc lithosphere, all formed above a Jurassic, northward-dipping subduction zone (figure 14). Because there are such complex variations, however, a final interpretation will require detailed tectonic and petrological study of all the ophiolite fragments within the belt.

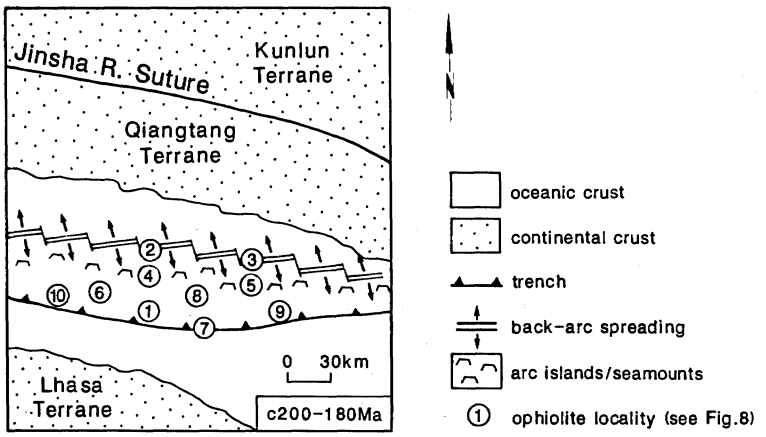

FIGURE 14. Schematic simplified reconstruction of the Jurassic tectonic setting of the Banggong–Nujiang ophiolite belt showing possible environments of formation of the various ophiolite fragments.

5. JINSHA RIVER OPHIOLITE BELT

(*a*) *Geology*

The Jinsha River (also known as the Hoh Xil-Yushu) ophiolite belt is the third ophiolite belt and lies on the Jinsha River Suture between the Qiangtang and Kunlun Terranes. Preliminary data from two ophiolites are reported here: at Bayinchawuma located about 100 km west of

the geotraverse road at Erdaogou; and at Yushu to the east near the Tongtian River on the Qinghai–Sichuan border (figure 1).

The map of the Bayinchawuma ophiolite made by the Geological Team of Qinghai Province is shown in figure 15. Two ophiolite outcrops were recognized, both comprising totally serpentinized harzburgites containing antigorite, bastite and magnetite as alteration minerals and primary chrome spinel, and forming klippen within the Triassic Batang Group.

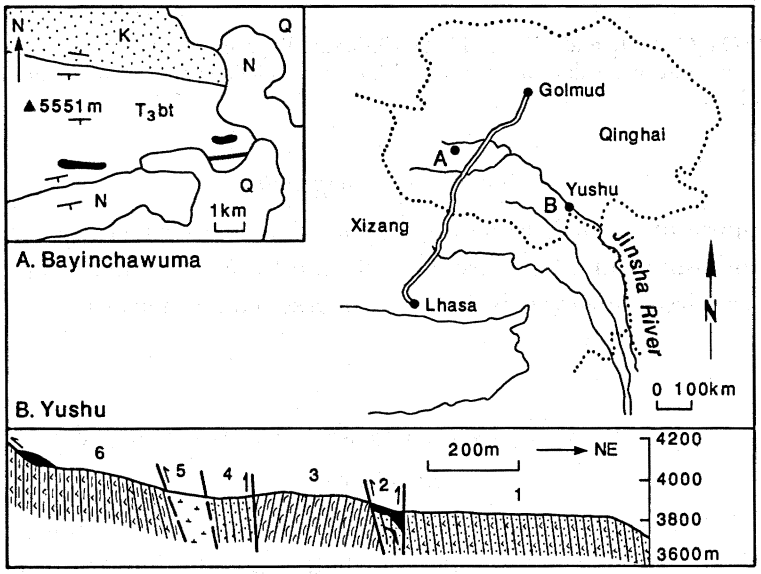

FIGURE 15. Geological maps and sections of the Bayinchawuma and Yushu ophiolite localities in the Jinsha River ophiolite belt. In map A, ophiolite outcrops are shown in black, T_3bt is the Triassic Batang group (sandstone, phyllites, tuffs and bioclastic limestone), K is the Cretaceous Fenguoshan Group (redbeds) and N and Q are Neogene and Quaternary deposits respectively. In section B (taken from Pan 1984), 1 = Batang Group, 2 = peridotites, 3 = pillow basalts and picrites, 4 = siliceous rocks, 5 = gabbros and 6 = tuff slates.

The Yushu ophiolite, discovered by Pan (1984) near the Tongtian River and not visited on the Geotraverse, consists of a disrupted sequence of ultramafic rocks (not showing tectonic fabrics; Pan, pers. comm.), gabbros, pillow basalts and picrites, and associated tuffs and cherts distributed as blocks within the Batang group (figure 15). All rocks are strongly altered, the pillow lavas to greenschists and amphibolites.

(*b*) *Petrology and geochemistry*

Few data exist from this ophiolite belt: spinels from the Bayinchawuma ophiolite are being analysed at the time of writing while only major element data are available for the Yushu ophiolite. Despite limited immobile element data, the Yushu ophiolite can be seen probably to have a MORB chemistry: lava compositions fall consistently within the MORB field of both the Ti–Cr and $FeO/MgO–TiO_2$ discrimination diagrams (figure 16) and the apparent crystallization history is olivine, plagioclase, clinopyroxene.

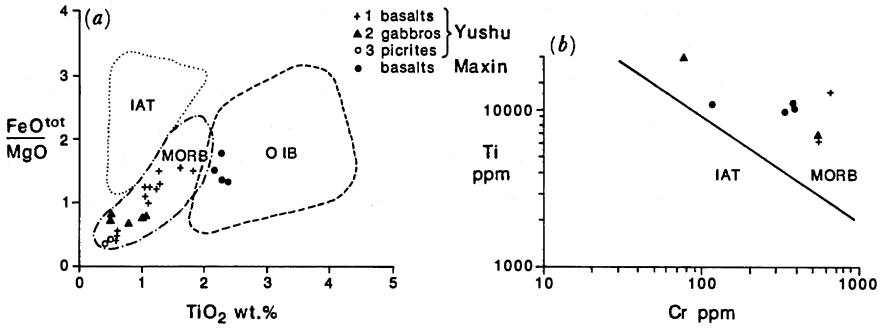

FIGURE 16. (*a*) FeO/MgO–TiO_2 and (*b*) Cr–Ti discriminant diagrams for lavas from the Yushu and Maxin ophiolites. MORB = mid-ocean ridge basalts; IAT = island arc tholeiites; and OIB = ocean island basalts. For full analyses see table 4.

(*c*) *Tectonic interpretation*

The MORB composition of the Yushu ophiolite points to an origin either in a major (incipient or evolved) ocean basin or in a back-arc basin distant from its related subduction zone. More data are clearly required, however, before any concrete conclusions can be drawn for the belt as a whole.

6. ANYEMAQEN-JISHISHAN OPHIOLITE BELT

(*a*) *Geology*

This ophiolite belt was not studied during the Geotraverse. It is, however, important to understand its origin because of the question of whether an additional Suture should be drawn within the Kunlun Terrane. The best-studied ophiolite of this belt is the Maxin ophiolite in eastern Qinghai province (figure 17). The complex occurs in a 30 km-wide NW–SE trending belt within lower Permian bioclastic limestone and associated silty slates, tuffs and basalts. The ophiolite is mainly composed of highly serpentinized and tectonized peridotites, mostly harzburgites but with some lherzolites, which crop out as lenses of varying sizes. Other members of the ophiolite series have not yet been found, although pillow lavas are found possibly interbedded with lower Permian marble.

(*b*) *Petrology and geochemistry*

The peridotites are characterized by 'fertile' compositions, notably high Al_2O_3 and residual clinopyroxene, which indicate that a supra-subduction zone origin is unlikely. The lavas contain some microphenocrysts of clinopyroxene in a groundmass of volcanic glass, plagioclase microlites and clinopyroxene, variably altered to a chlorite, calcite, sericite assemblage; some typical analyses are given in table 4. These data confirm the non-subduction related character, plotting in the MORB field of the immobile element discrimination diagram, Ti–Cr (figure 16*b*). The FeO/MgO–TiO_2 diagram (figure 16*a*) further indicates that the analyses may be of within-plate tholeiite or plume-related (P-type) MORB composition and this interpretation is supported by rare-earth analyses, which show LREE enrichment (figure 18). Comparable compositions are found at the present day in some oceanic islands, or seamounts (e.g. Hawaii, Iceland) and in areas of strongly attenuated continental lithosphere (e.g. Afar).

PHILOSOPHICAL TRANSACTIONS OF THE ROYAL SOCIETY A MATHEMATICAL, PHYSICAL & ENGINEERING SCIENCES

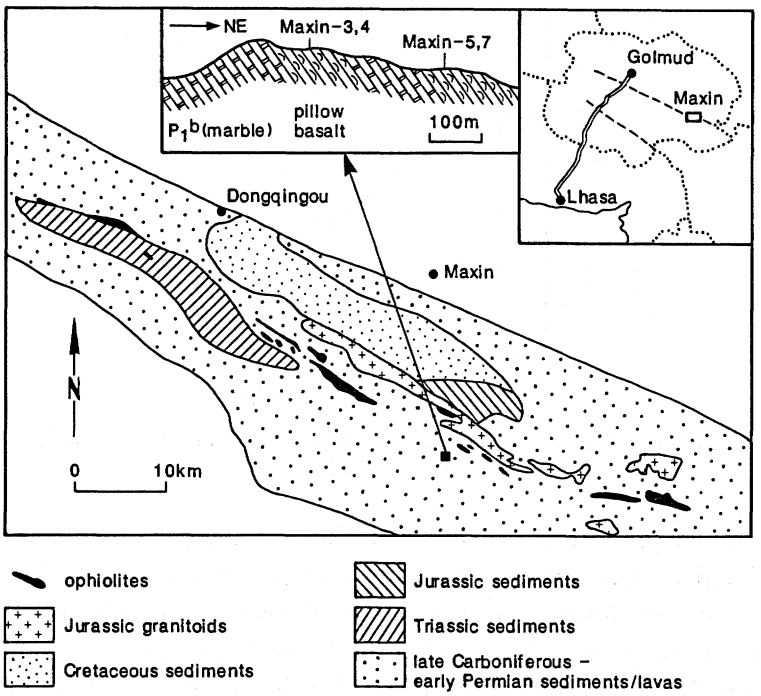

FIGURE 17. Geological map of the Anyemaqen–Jishi mountain ophiolite belt.

TABLE 4. REPRESENTATIVE MAJOR ELEMENT ANALYSES OF BASIC ROCKS FROM THE JINSHA RIVER (YUSHU) AND ANYEMAQEN–JISHI (MAXIN) MOUNTAIN OPHIOLITE BELTS

sample	Yushu	Yushu	Yushu	Yushu	Yushu	Maxin	Maxin	Maxin	Maxin
location	Y-71	Y-79	Y-123	Y-81	Y-107	Maxin3	Maxin4	Maxin5	Maxin7
rock	pic.	gab.	gab.	bas.	bas.	bas.	bas.	bas.	bas.
type	L	Int.	Int.	PL	PL	PL	PL	PL	PL
SiO_2	43.17	48.43	48.35	48.41	44.24	47.25	46.14	46.18	47.05
TiO_2	.25	1.14	3.94	1.20	1.96	2.34	2.19	2.40	2.28
Al_2O_3	6.44	13.47	14.13	14.14	11.37	13.96	13.60	13.15	14.53
Fe_2O_3	13.55	9.22	11.55	8.98	12.90	10.02	10.61	9.71	10.51
MnO	.18	.24	.16	.18	.17	.14	.16	.16	.18
MgO	31.82	7.93	4.44	7.90	12.01	7.77	7.80	7.78	6.39
CaO	2.80	12.93	6.50	11.60	8.18	8.94	10.76	9.59	8.35
Na_2O	.07	2.87	3.56	2.57	.83	3.07	2.84	3.01	3.61
K_2O	.09	.30	1.98	.37	.19	.36	.51	1.06	.80
P_2O_5	.01	.13	.48	.11	.26	.33	.32	.44	.38
LOI	0.00	2.84	3.04	3.05	5.22	4.12	3.94	4.66	3.97
Total	98.38	99.50	98.13	98.51	97.33	98.30	98.87	98.14	98.05
Cr	3600	600	90	500	610	370	351	371	185

Key to rock types: pic. = picrite; gab. = gabbro; bas. = basalt ; L = massive lava; Int. = intrusion; PL = pillow lava.

(*c*) *Interpretation*

The geochemical evidence that the lavas are not of typical ocean ridge type is consistent with the field evidence of possible interbedding with limestone which supports the seamount or attenuated continental lithosphere hypotheses. Possible analogues have been found at the margins of the Red Sea (Coleman 1984) and on the Red Sea island of Zabargad, where

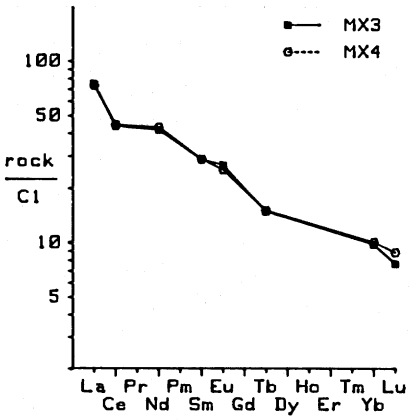

FIGURE 18. Chondrite-normalized rare-earth patterns of two lavas from the Anyemaqen-Jishi mountain ophiolite belt.

peridotites are exposed (Bonatti *et al.* 1981). If such analogies do hold, the ophiolites could represent transitional or immature oceanic lithosphere formed during Permian rifting and emplaced during Triassic closure. There is, as yet, however, no evidence that true oceanic lithosphere existed in the area. In relation to the Geotraverse, it is possible that some of the cumulate igneous rocks found in clasts in glacial moraine along the Kunlun fault formed in a similar setting and are of similar age to the Maxin ophiolite, although their most probable origin is intrusive, related to the post-kinematic Kunlun plutonic complexes (Kidd & Molnar, this volume). Even if this is the case, however, we consider it valid to treat the Kunlun Terrane as a single Terrane (Chang *et al.* 1986), at least until evidence for true oceanic lithosphere is found.

7. SUMMARY AND CONCLUSIONS

The principal conclusions of this study can be summarized as follows.

1. Our data confirm previous interpretations that the ophiolites of the Yarlung–Zangbo Suture are of MORB composition and that they represent anomalous Cretaceous oceanic lithosphere formed within the neo-Tethyan ocean. The lower-than-normal crustal thickness, presence of intra-oceanic unconformities and melanges, presence of 'fertile' peridotites, and late intrusion of dykes and sills of MORB composition into already-formed lithosphere may indicate the importance of ridge-transform intersections in the origin of the ophiolite, an interpretation in line with reconstructions requiring short north–south ridge segments offset by major transform faults.

2. Our data also confirm previous interpretations that the ophiolites associated with the Banggong Suture formed in supra-subduction zone environments. The chemical zonation of lavas and dykes is used further to suggest that the ophiolitic fragments are derived from an arc-basin complex developed above a Jurassic northward-dipping subduction zone, those in the south representing fore-arc lithosphere, those in the central zone representing island arc or arc seamount lithosphere and those in the north representing back-arc lithosphere. MORB-lithosphere appears to be present in one locality, in the Ado Massif. Ophiolite emplacement may have taken place in at least two stages: a continent-arc or continent-fore-arc collision event in the Jurassic; and a continent-continent collision event in the Cretaceous.

3. There is insufficient evidence to make a full interpretation of the tectonic setting of

formation of the ophiolites of the Jinsha River Suture zone. One of the best-studied ophiolites in the zone, the Yushu ophiolite east of the Geotraverse, is of MORB composition, while the Bayinchawuma ophiolite just west of the Geotraverse route comprises strongly depleted harzburgites and may be of supra-subduction zone character.

4. The Anyemaqen–Jishi mountain ophiolite belt east of the Kunlun mountains contains, at Maxin, tectonised peridotites and pillow lavas with within-plate tholeiite character which may have belonged to transitional or immature oceanic lithosphere, but which do not constitute sufficient evidence for placing an additional Suture within the Kunlun Terrane.

We should like to thank: Ernesto Abbate, Costas Xenophontos and members of the Geotraverse team for helpful discussions; Zhang Kiuwu, Zhang Qi and the Geological Team of Qinghai Province for mapping and sampling the Bayinchawuma ophiolite after our own attempt failed; and Peter Oakley, Peter Murray, Nick Rogers, Yang Ruiyang and Liu Jialin for analytical work.

References

Bonatti, E., Hamlyn, P. R. & Ottonello, G. 1981 The upper mantle beneath a young oceanic rift: peridotites from the island of Zabargad (Red Sea). *Geology* **9**, 474–479.

Chang Chengfa *et al.* 1986 Preliminary conclusions of the Royal Society and Academia Sinica 1985 geotraverse of Tibet. *Nature, Lond.* **323**, 501–507.

Cherchi, A. & Schroeder, R. 1980 *Palorbitolinoides hedini* n. gen. n. sp. grand foraminifère du Crétacé inf. du Tibet meridional. *C.r. Acad. Sci., Paris* **291**, 385–388.

Coleman, R. G. 1984 The Tahama Asia igneous complex, a passive margin ophiolite. *27th Internat. Geol. Congress, Moscow* **23**, 93–121.

Deng Wanming 1981 A preliminary study of the petrology and genesis of the Yarlung Zangbo ophiolite belt. In *Proceedings of Symposium on Qinghae-Xizang (Tibet) Plateau (Beijing, China)*, pp. 529–538. New York Science Press; Gordon & Breach.

Deng Wanming 1982 Studies on the igneous petrology of the Yarlung-Zangbo ophiolite, Xizang. In *Proceedings of geological research or Qinghai-Xizang*, pp. 36–52. Beijing Geological Publishing House. (In Chinese.)

Deng Wanming 1983 Geological comparison between the ultrabasic rock belts in Northern and Southern Xizang. *Petr. Res.* **3**, 1–16. (In Chinese.)

Deng Wanming 1984 Petrogenesis of the basic-ultrabasic rock belt along Dongqiao-Nujiang in Northern Xizang (Tibet). *Himalayan Geology* **II**, 81–98. (In Chinese.)

Deng Wanming & Zhou Yusheng 1982 Geological evolution of oceanic crust in Mesozoic eastern Tethys as exemplified by the Yarlung-Zangbo ophiolite zone. *IGAS Research on Geology*, pp 42–48. (In Chinese.)

Deng Wanming, Yang Ruiyang, Huang Zhongxiang, Jiang Yong, Guo Yinghun, Luo Shihua, Zhao Zhenlan & Feng Xizhang 1984 Trace element geochemistry of the ophiolite complex in the Xigaze district, Xizang. In *Sino-French co-operative investigation in Himalayas*, pp. 221–237. Beijing Geological Publishing House. (In Chinese.)

Deng Wanming, Yang Ruiyang & Huang Zhongxiang 1985 Trace element characteristics of the mafic-ultramafic plutons in Northern Xizang. *Petr. Res.* **6**, 47–58.

Dick, H. J. B. & Bullen, T. 1984 Chromium spinel as petrogenetic indicator in abyssal and Alpine type peridotites and spatially associated lavas. *Contr. Miner. Petr.* **86**, 54–76.

Dietrich, V., Emmermann, R., Oberhansli, R. & Puchelt, H. 1978 Geochemistry of basaltic and gabbroic rocks from the West Mariana Basin and the Mariana Trench. *Earth planet. Sci. Lett.* **39**, 127–144.

Fox, P. J. & Straup, J. B. 1981 The plutonic foundation of the oceanic crust. In *The Oceanic lithosphere. The Sea*, VIII (ed. C. Emiliani), pp. 119–218.

Girardeau, J., Marcoux, J., Allègre, C. J., Bassoullet, J. P., Tang Youking, Xiao Xuchang, Zao Yougong & Wang Xibin 1984 Tectonic environment and geodynamic significance of the Neo-Cimmerian Dongqiao ophiolite, Banggong-Nujiang Suture zone, Tibet. *Nature, Lond.* **307**, 27–31.

Girardeau, J., Mercier, J.-C. C. & Zao Yougong 1985*a* Origin of the Xigaze ophiolite, Yarlung Zangbo Suture zone, Southern Tibet. *Tectonophysics* **119**, 407–433.

Girardeau, J., Mercier, J.-C. C. & Wang Xibin 1985*b* Petrology of the mafic rocks of the Xigaze ophiolite, Tibet. *Contr. Miner. Petr.* **90**, 309–321.

Girardeau, J., Marcoux, J, Fourcade, E., Bassoullet, J. P. & Tang Youking 1985*c* Xainxa ultramafic rocks, central Tibet, China; tectonic environment and geodynamic significance. *Geology* **13**, 330–333.

Glassley, W. 1974 Geochemistry and tectonics of the Crescent Volcanic rocks, Olympia Peninsula, Washington. *Bull. geol. Soc. Am.* **85**, 785–794.

PHILOSOPHICAL TRANSACTIONS OF THE ROYAL SOCIETY A MATHEMATICAL, PHYSICAL & ENGINEERING SCIENCES

Göpel, C., Allègre, C. J. & Xu Ronghua 1984 Lead isotope study of the Xigaze ophiolite (Tibet): the problem of the relationship between magmatites (gabbros, dolerites, lavas) and tectonites (harzburgites). *Earth planet. Sci. Lett.* **69**, 301–310.

Hawkins, J. W. & Melchior, J. T. 1985 Petrology of the Mariana Trough and Lau Basin basalts. *J. geophys. Res.* **90**, 11431–11468.

Ishiwatari, K. 1985 Alpine ophiolite: product of low-degree mantle melting in a Mesozoic transcurrent rift zone. *Earth planet. Sci. Lett.* **76**, 93–108.

Leterrier, J., Maury, R. C., Thonon, P., Girard, D. & Marchal, M. 1982 Clinopyroxene composition as a method of identification of the magmatic affinities of palaeo-volcanic series. *Earth planet. Sci. Lett* **59**, 139–154.

Marcoux, J., De Wever, P., Nicolas, A., Girardeau, J., Xiao Xuchang, Chang Chengfa, Wang Naiwen, Zao Yougong, Bassoullet, J. P., Colchen, M. & Mascle, G. 1982 Preliminary report on depositional sediments on top of the volcanic member: the Xigaze ophiolite (Yarlung-Zangbo suture zone). *Ofioliti* **2/3**, 395–396.

Molnar, P. & Tapponnier, P. 1975 Cenozoic tectonics of Asia: effects of a continental collision. *Science, Wash.* **189**, 419–426.

Nicolas, A., Girardeau, J., Dupré, B., Wang Xibin, Zheng Haixiang, Zao Yougong & Xiao Xuchang 1981 The Xigaze ophiolite: a peculiar oceanic lithosphere. *Nature, Lond* **294**, 414–417.

Nisbet, E. G. & Pearce, J. A. 1977 Clinopyroxene composition in mafic lavas from different tectonic settings. *Contr. Miner. Petr.* **63**, 149–180.

Pan Yusheng 1984 Ophiolite suite was discovered in Tongtian River, Qinghai Province. *Seismol. Geol.* **6**, 44–58.

Pearce, J. A. 1975 Basalt geochemistry used to investigate past tectonic environments on Cyprus. *Tectonophysics* **25**, 41–67.

Pearce, J. A. 1982 Trace element characteristics of lavas from destructive plate boundaries. In *Andesites* (ed. R. S. Thorpe), pp. 525–547. Chichester: J. Wiley and Sons.

Pearce, J. A. & Cann, J. R. 1973 Tectonic setting of basic volcanic rocks determined using trace element analysis. *Earth planet. Sci. Lett.* **19**, 290–300.

Pearce, J. A., Lippard, S. J. & Roberts, S. 1984 Characteristics and tectonic significance of supra-subduction zone ophiolites. In *Marginal Basin. Geology* (ed. B. P. Kokelaar & M. F. Howells), *Geol. Soc. Lond. Spec. Publ.* 16, pp. 77–93.

Pozzi, J. P., Westphal, M., Girardeau, J., Besse, J. & Zhou Yaoxiu 1984 Palaeomagnetism of the Xigaze ophiolite and flysch: latitude and direction of spreading. *Earth planet. Sci. Lett* **70**, 383–394.

Prinzhofer, A., Allègre, C. J., Bao Peisheng & Wang Xibin 1984 Magmatism in southern Tibet: trace element constraints. In *Himalayan Geology. Chengdu Int. Symp. 1984.* Beijing Academia Sinica (abstr.).

Rogers, N., MacLeod, C. J. & Murton, B. J. (in press). Petrogenesis of boninitic lavas from the Limassol Forest Complex, Cyprus.

Sengör, A. M. C. 1981 The geological exploration of Tibet. *Nature, Lond.* **294**, 403–404.

Tang Youking & Wang Fangguo 1984 Primary analysis of the tectonic environment of the ophiolite in Northern Xizang. *Himalayan Geology* **II**, 99–113. (In Chinese.)

Wang Xibin, Bao Beishang & Zheng Haixiang 1984 A structurally disrupted ophiolite in the Lake area of Northern Xizang (Tibet) and its geochemistry. *Himalayan Geology* **II**, 112–141. (In Chinese.)

Wood, D. A., Joron, J.-L. & Treuil, M. 1979 A re-appraisal of the use of trace elements to classify and discriminate between magma series erupted in different tectonic settings. *Earth planet. Sci. Lett.* **45**, 326–336.

Wu Huarao & Deng Wanming 1980 Basic geological features of the Yarlung Zangbo ophiolite belt, Xizang, China. In *Ophiolites* (ed. A. Panayiotou), pp. 462–472. Nicosia Cyprus Geological Survey.

Yang Ruiyang & Deng Wanming 1986 Trace element characteristics of the volcanics in the North Xizang. *Nuclear Techniques* **2**, 17–20. (In Chinese.)

Zhang Qi & Yang Ruiyang 1986 The boninite-like pluton in ophiolite from Dengqen, Xizang, and its geological significance. *Kexue Tongbao* **31**, 405–408.

PHILOSOPHICAL TRANSACTIONS OF THE ROYAL SOCIETY A MATHEMATICAL, PHYSICAL & ENGINEERING SCIENCES